Physica C 470 (2010) 129–133

Contents lists available at ScienceDirect

Physica C

journal homepage: www.elsevier.com/locate/physc

Heat treatment effect on the strain dependence of the critical current for an internal-tin processed Nb_3Sn strand

Sangjun Oh *, Soo-Hyeon Park, Chulhee Lee, Heekyung Choi, Keeman Kim

National Fusion Research Institute, 52 Eoeun-dong, Yuseong, Daejeon 305-333, Republic of Korea

ARTICLE INFO

Article history:
Received 3 July 2009
Received in revised form 16 October 2009
Accepted 6 November 2009
Available online 17 November 2009

Keywords:
Heat treatment
Internal-tin Nb_3Sn
Scaling law for flux pinning
Strain dependence of the critical current

ABSTRACT

A comparative study on the effects of heat treatment, especially, the duration of the A15 reaction temperature plateau on the strain dependence of the critical current for an internal-tin processed Nb_3Sn strand has been carried out. The strain dependence of the critical current is measured by a variable temperature Walter spiral probe that we have developed. It was shown that prolonged heat treatment can be a very effective way to improve the strain dependency. For a quantitative analysis, the measured data were analyzed with various proposed scaling laws: the scaling law based on strong-coupling theory, the modified deviatoric strain scaling law, and the interpolative scaling law. We found that there is a slight increase in the critical temperature and a substantial improvement in the maximum pinning force. The origin of improved strain dependency is further discussed.

1. Introduction

The superconducting properties of Nb_3Sn strongly depend on the atomic percent of Sn [1,2]. For example, the critical temperature of Nb_3Sn is around 6 K if the amount of Sn is below 20%. As the Sn content is increased, the critical temperature sharply increases and saturates at about 18 K when the atomic percent of Sn is above 24.5%. The upper critical field is also strongly affected by the variation of Sn content. The upper critical field increases almost linearly from 5 T to around 30 T as the Sn content varies from 19.5% to 24.5%, and then decreases sharply with a further increment of Sn. It is reported that a structural transition occurs from the cubic to the tetragonal phase when the Sn content is about 24.5%. There can be thousands of filaments as small as a few micrometers in diameters within a commercial Nb_3Sn strand. Nb_3Sn strands are usually heat treated at temperatures between 650 and 700 °C for periods exceeding 100 h in order to optimize their properties. However, compositional variation within each filament or among filaments is inevitable during the solid state reaction by the diffusion process and there can even be an un-reacted Nb core region [2]. Not only the fundamental superconducting properties, such as the transition temperature or the upper critical field, as discussed above, but also the size and shape of grains depend on the heat treatment conditions. There are several reports on the heat treatment dependence of various properties such as the transition temperature, the upper critical field, the residual resistance ratio, the critical current, and even the AC loss [3–5]. On the other hand, the heat treatment effect on the strain dependence of the critical current has been rarely reported. For large scale applications, such as the International Thermonuclear Experimental Reactor (ITER) magnetic coils, the strain on Nb_3Sn strands during operating conditions can be as high as −0.8% [6] and the critical current can be reduced to more than a half of its maximum value. A slight improvement in the strain dependence of the critical current can be critically beneficial for the overall performance of the magnetic coils. In this work, the effect of heat treatment conditions, especially, the duration time at the A15 reaction temperature on the strain dependence of the critical current for an internal-tin processed wire has been studied. The wire studied is a possible candidate strand for the ITER magnetic coils. For a more solid comparison, the measured data are analyzed with various recently proposed scaling laws.

2. Experimental

Fig. 1a shows an optical microscope image before heat treatment for the internal-tin Nb_3Sn strand studied in this work. The strand was manufactured by Kiswire Advanced Technology (KAT) and contains about 2 wt.% of Ti. The outer diameter is 0.82 mm, the number of filaments is 3344, and the average filament diameter is about 5.5 μm. Samples were heat treated with a ramp rate of 5 °C/h. For the first sample, hereafter referred to as sample 100 h, the heat treatment was carried out at 210 °C for 50 h, 340 °C for 25 h, 450 °C for 25 h, 575 °C for 100 h, and finally at 650 °C for 100 h. The second sample, hereafter referred to as sample 150 h, was reacted by exactly the same way except the duration time at 650 °C. The second sample was heat treated at

* Corresponding author. Address: Material Research Team, National Fusion Research Institute, 52 Eoeun-dong, Yuseong, Daejeon 305-333, Republic of Korea. Tel.: +82 42 870 1630; fax: +82 42 870 1939.
E-mail address: wangpi@nfri.re.kr (S. Oh).

0921-4534/$ - see front matter © 2009 Elsevier B.V. All rights reserved.
doi:10.1016/j.physc.2009.11.062

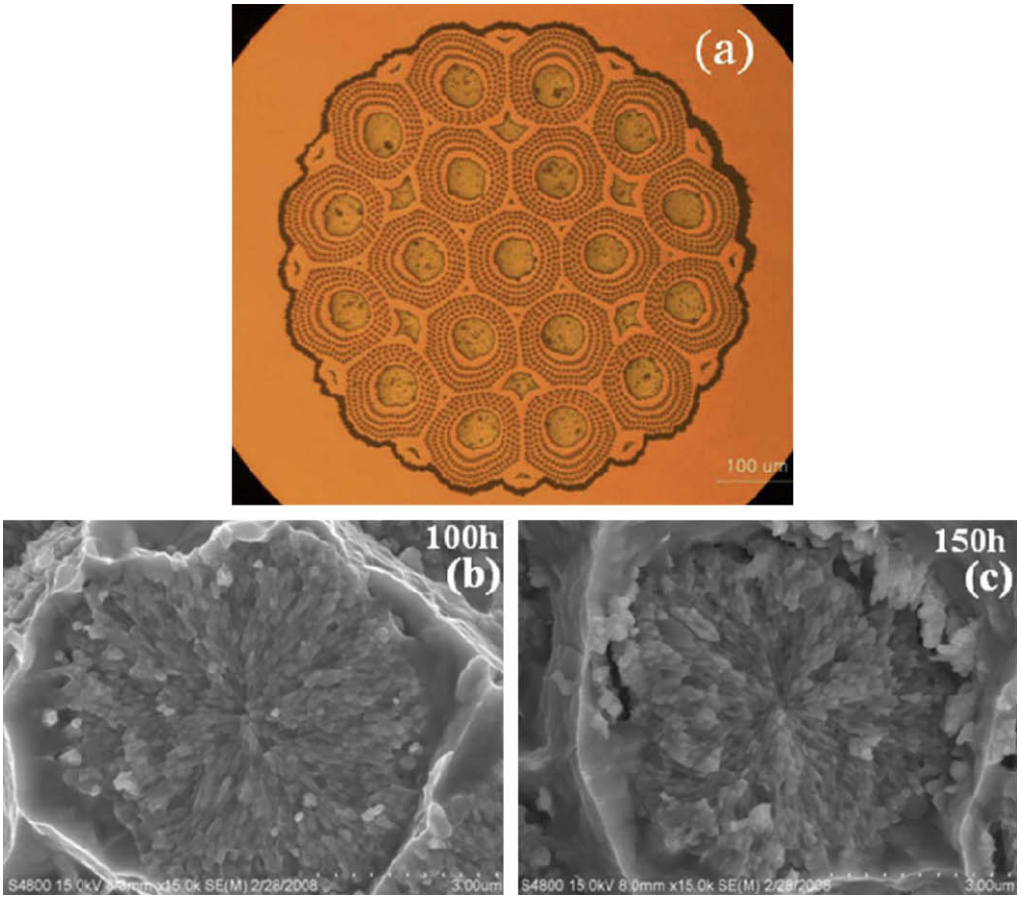

Fig. 1. Optical microscope and FE-SEM images before and after heat treatment for a KAT internal-tin processed Nb_3Sn strand.

650 °C for 150 h. The strain dependence of the critical current was measured by a variable temperature Walter spiral probe developed for this purpose. After the heat treatment, samples were transferred to beryllium copper spirals and were soldered. The beryllium copper spiral was twisted back and forth. Both tensile and compressive strain could be reversibly applied to the strand up to 0.7%. Three temperature sensors were attached to the spiral and the temperature was controlled within ±50 mK during the critical current measurement up to 80 A. Details of measurement procedure are reported in our previous works [7,8].

3. Results and discussion

No noticeable difference in the microstructure is observed by the variation of heating duration at the A15 reaction temperature from 100 to 150 h as can be seen in the Field Emission Scanning Electron Microscope (FE-SEM) images shown in Fig. 1b and c. No un-reacted Nb core was found for both samples and the overall grain shape within each filament seemed to be similar. However, there was an obvious improvement in the critical current density. For example, the critical current maximum at 4.2 K, 8 T increased from 496.1 to 513.3 A with 50 h of additional heat treatment at 650 °C. The critical current of each sample at various fields, temperatures, and strains is shown in Fig. 2. The increment of the normalized critical current is not uniform as can be more clearly seen in Fig. 3. The normalized critical current as a function of applied strain for three different fields and temperatures is presented in Fig. 3. In the tensile strain region, the strain dependence of the critical current is approximately the same for both samples. In the compressive strain region, the strain dependence is improved by the prolonged heat treatment. The amount of improvement is dependent on both field and temperature. It is relatively small at low field and temperature (for example, at 4.2 K, 9 T). But notable improvement is observed as the field and the temperature are increased.

The measured results were analyzed by recent scaling laws for flux pinning, for a quantitative comparison. Among various scaling laws proposed [9–11], the scaling law based on the strong-coupling theory of superconductivity [9] is of interest. In that scaling law the strain dependence of the critical current can be decomposed into and can be attributed to three superconducting parameters; (a) the strain dependence of the critical temperature, which can be written as, $T_c(\varepsilon) = T_c(0)(1-\alpha|\varepsilon|^{1.7})$, (b) the thermodynamic critical field, $B_c(0,\varepsilon) = B_c(0,0)(1-\beta|\varepsilon|^{1.7})$ and (c) the Ginzburg–Landau parameter, $\kappa(0,\varepsilon) = \kappa(0,0)(1-\gamma|\varepsilon|^{1.7})$ [9]. Intrinsic strain (ε) is defined as, $\varepsilon = \varepsilon_{app} - \varepsilon_m$, a difference between the applied (ε_{app}) and the maximum strain (ε_m) where the maximum values of superconducting parameters are reached. The coefficients α, β and γ describe the strain dependency of each superconducting parameter. The upper critical field, B_{c2}, can be obtained from the relation: $B_{c2} = \sqrt{2}B_c \cdot \kappa$. The pinning force maximum, F_m, can be calculated using the Kramer model [12]:

$$B_{c2}(T,\varepsilon) = B_{c2}(0,0)(1-\beta|\varepsilon|^{1.7})(1-\gamma|\varepsilon|^{1.7})(1-t^{2.17})k(t,\varepsilon)$$
$$F_m(T,\varepsilon) = F_m(0,0)(1-\beta|\varepsilon|^{1.7})^{5/2}(1-\gamma|\varepsilon|^{1.7})^{1/2}(1-t^{2.17})^{5/2}k(t,\varepsilon)^{1/2} \quad (1)$$

where

$$k(t,\varepsilon) = \left(1+u\frac{1-\gamma|\varepsilon|^{1.7}}{1-\alpha|\varepsilon|^{1.7}}(1-t^{v})\right)\Big/\left(1+u\frac{1-\gamma|\varepsilon|^{1.7}}{1-\alpha|\varepsilon|^{1.7}}\right)$$

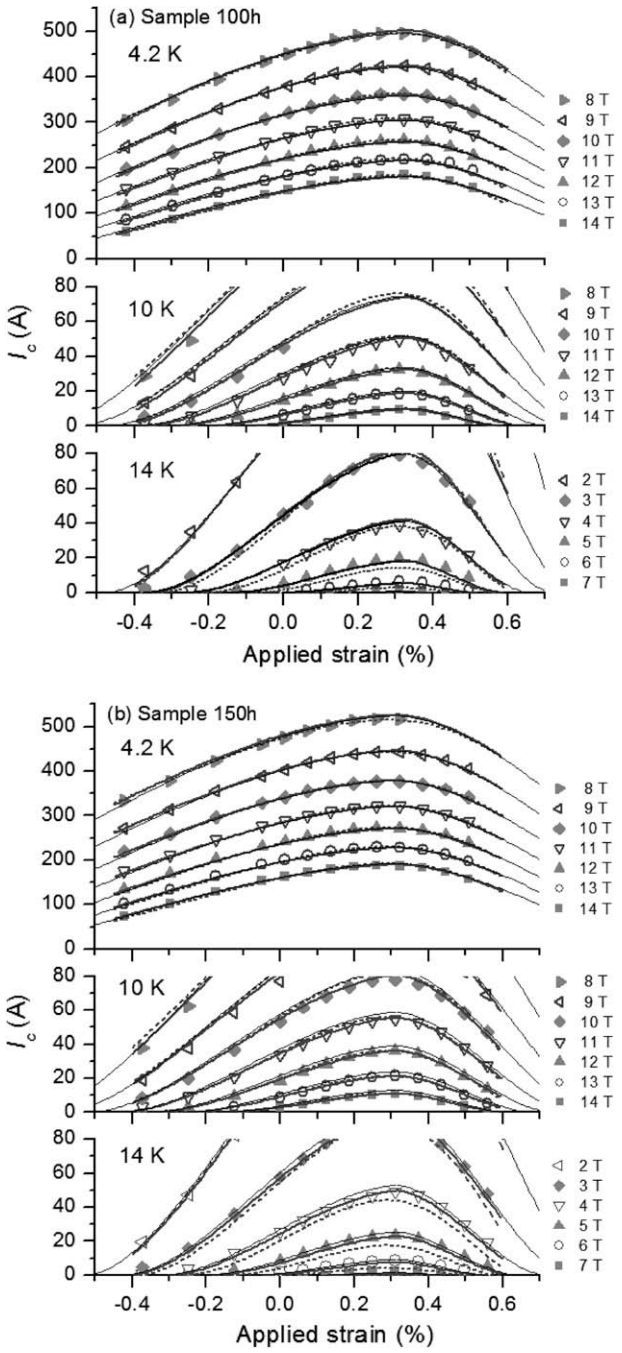

Fig. 2. The field, temperature and strain dependence of the critical current for the KAT internal-tin processed Nb_3Sn strand with different heat treatment scenarios. Solid lines were calculated with Eq. (2), the scaling law based on strong-coupling theory and dotted lines were calculated with Eq. (3), the modified deviatoric scaling law.

The reduced temperature is defined as, $t = T/T_c$ and the other fitting parameters, u and v are related to the temperature dependence of the superconducting parameters. The critical current can be written as [9],

$$I_c(B,T,\varepsilon) = (F_m(T,\varepsilon)/B)\cdot b^{1/2}(1-b)^2 \quad (2)$$

where b is the reduced field, $b = B/B_{c2}$.

The thin solid lines in Fig. 2 were calculated with Eq. (2). First, the strain and temperature dependences of the upper critical field

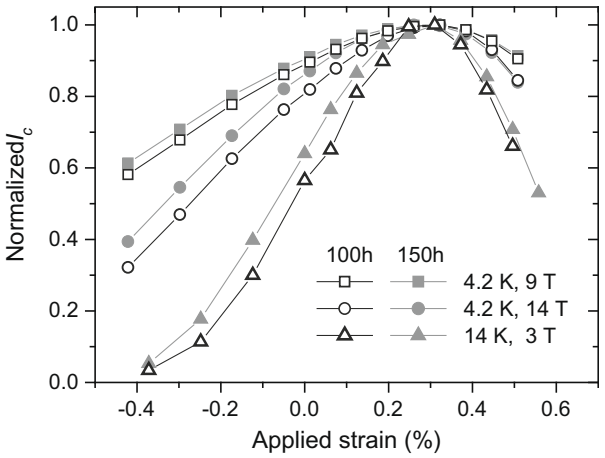

Fig. 3. Normalized I_c as a function of applied strain for the samples 100 h and 150 h at various fields and temperatures.

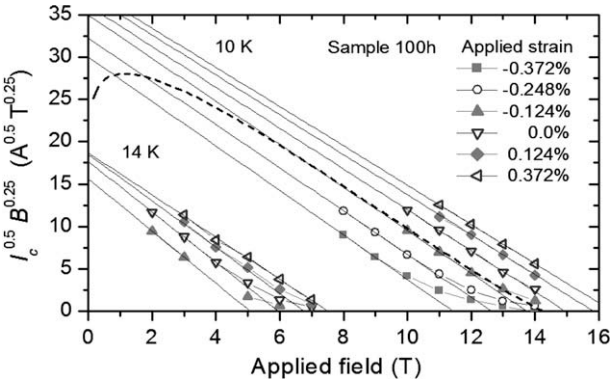

Fig. 4. Kramer plots for the sample 100 h at 10 and 14 K. Solid lines are the Kramer extrapolations and the dotted line corresponds to $b^{0.697}(1-b)^{2.266}$.

and the pinning force maximum are obtained from Kramer plots by linear extrapolation. The Kramer plots for the sample 100 h are shown in Fig. 4 as an example. The positive curvature near the upper critical current might be understood in correlation with the field dependence of the n-value [13]. However, it is not considered here for simplicity as was discussed in our previous work [8]. The extracted upper critical field and the pinning force maximum are presented in Fig. 5. The solid lines in Fig. 5 were calculated with Eq. (1). All the fitting parameters needed for the calculation of the critical current with Eq. (2) are obtained from the fitting of the extracted upper critical field and the pinning force maximum, as listed in Table 1. The fitting parameters for the temperature dependency, u and v not listed in Table 1 were 0.85 and 1.2, respectively.

By an increase in the heat treatment duration time, a slight increase in the transition temperature and a substantial increment in the pinning force maximum are observed. On the other hand, the Ginzburg–Landau parameter strain dependency coefficient γ is significantly lowered whereas there is a slight increment in the thermodynamic strain coefficient β, which seems to be a main cause for the observed difference in the overall stain dependence of the critical current. The coefficient, α which is related to the strain dependence of the critical temperature is almost the same for both samples 100 h and 150 h in the compressive strain region but is much lower for sample 150 h in the tensile strain region. Microscopically, α and β are related to the strain dependence of the electron–phonon spectrum density function, whereas γ is also dependent on the level of the impurity scattering [9]. It might be

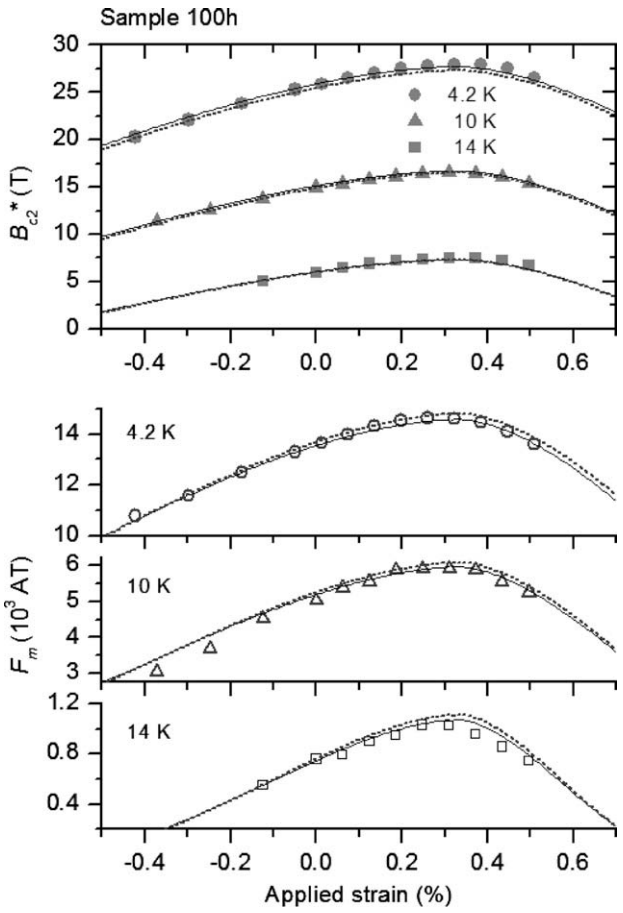

Fig. 5. The pinning force maximum as a function of temperature and strain for the sample 100 h.

Table 1
Fitting parameters obtained with Eq. (1) for samples 100 h and 150 h.

α	β	γ	ε_m(%)	T_c(0) (K)	B_{c2}(0,0) (T)	F_m(0,0) (AT)
100 h $\varepsilon < \varepsilon_m$						
450	280	750	0.33	17.2	31.8	17,200
$\varepsilon > \varepsilon_m$						
1250	850	1400	0.33	17.2	31.8	17,200
150 h $\varepsilon < \varepsilon_m$						
450	350	650	0.314	17.4	31.8	18,100
$\varepsilon > \varepsilon_m$						
950	900	1300	0.314	17.4	31.8	18,100

argued that the prolonged heat treatment affects the impurity scattering and that is a major cause of improved strain dependency in the compressive strain region. On the other hand, there is an additional effect of the electron–phonon spectrum in the tensile region which mitigates the overall strain dependence of the critical current in the tensile strain region.

As there can be some arbitrariness in the determination of the parameters, the critical current was directly fitted by a non-linear least square fit with Eq. (2). Previously, the critical current was indirectly analyzed from the fitting of the extracted upper critical field and the pinning force maximum. Here, u and v were not used as variable fitting parameters and were set to 0.85 and 1.2, respectively. A fixed temperature dependency coefficient was also used in a recent scaling law proposed by Godeke et al. [11]. The best fit is obtained with parameters listed in Table 2. The fitting parameters are quite similar to the previous results and give a slightly better fit to the measured critical current data as shown in Fig. 2 as thick solid lines. General trends in the fitting parameter variations with the change of the heat treatment condition are almost the same as before. The parameters obtained from the direct fitting do not necessarily need to fit the extracted upper critical field and the pinning force maximum, since there is some uncertainty in their determination from the Kramer plots. In this case, the direct fitting parameters also give reasonable fits to the strain and field dependence of the upper critical field and the pinning force maximum as can be seen in Fig. 5. Dotted lines are calculated with Eq. (1) using the parameters listed in Table 2.

Table 2
Fitting parameters obtained with Eq. (2) for samples 100 h and 150 h.

α	β	γ	ε_m(%)	T_c(0) (K)	B_{c2}(0,0) (T)	F_m(0,0) (AT)
100 h $\varepsilon < \varepsilon_m$						
461.5	300.2	731.1	0.333	17.24	31.3	17,454
$\varepsilon > \varepsilon_m$						
1301	833.7	1414	0.333	17.24	31.3	17,454
150 h $\varepsilon < \varepsilon_m$						
445.1	325.4	604.4	0.317	17.25	31.33	18,282
$\varepsilon > \varepsilon_m$						
958.6	909.9	1251	0.317	17.35	31.33	18,282

The critical current was analyzed further with other scaling laws recently proposed in order to see whether other scaling laws also give similar conclusions on the effect of the elongated heat treatment; a decrease in the strain dependency, a slight improvement in the critical temperature, and a substantial increment in the pinning force maximum. First, the measured results were analyzed with the scaling law recently proposed by Bottura [14]. It is based on the deviatoric scaling law proposed by Godeke et al. [11] and can be written as,

$$I_c(B,T,\varepsilon) = \frac{F_m(0,0)}{B} s(\varepsilon)(1-t^{1.52})(1-t^2)b^p(1-b)^q \tag{3}$$

where

$$s(\varepsilon) = 1 + \frac{1}{1-C_{a1}\varepsilon_{0,a}}\left[C_{a1}\left(\sqrt{\varepsilon_{sh}^2+\varepsilon_{0,a}^2} - \sqrt{(\varepsilon-\varepsilon_{sh})^2+\varepsilon_{0,a}^2}\right) - C_{a2}\varepsilon\right]$$

The parameters, C_{a1} and C_{a2} are the second and third invariant axial strain coefficient, respectively. The parameter, $\varepsilon_{0,a}$ is a remaining strain component. The parameter ε_{sh} is a shift due to the difference between the deviatoric and axial strain description and can be written as, $\varepsilon_{sh} = C_{a2}\varepsilon_{0,a}/\sqrt{C_{a1}^2 - C_{a2}^2}$. The critical temperature and the upper critical field can be written as, $T_c(\varepsilon) = T_c(0)s(\varepsilon)^{1/3}$ and $B_{c2}(T,\varepsilon) = B_{c2}(0,0)s(\varepsilon)(1-t^{1.52})$, respectively. A difference from the scaling law proposed by Godeke et al. is the allowance of variation in the parameters, p and q. In the scaling law of Godeke, p and q are fixed with 0.5 and 2, respectively, following the Kramer model.

The fitting parameters obtained from a non-linear least square fit on the measured critical current data with Eq. (3) are listed in Table 3. The best fit is obtained with values of p and q other than 0.5 and 2, which is the reason for the large difference in the fitting parameter value of $F_m(0,0)$ compared with the fitting result using the scaling law based on strong-coupling theory. If a function, $b^{0.697}(1-b)^{2.266}$ is represented in the form of a Kramer plot, there is a slight positive curvature near the upper critical field as shown in Fig. 4 as a dotted line. The calculated critical current data using the parameters listed in Table 3 are shown in Fig. 2 as dotted lines. With the lengthened heat treatment, both the second and third invariant axial strain coefficients, C_{a1} and C_{a2} decrease, which is a cause for the reduced strain dependency. Similar to the previous analysis, a small increase in the transition temperature or in the upper critical field and a huge increase in the pinning force maximum can be argued as well.

Table 3
Fitting parameters obtained with Eq. (3) for samples 100 h and 150 h.

p C_{a1}	q C_{a2}	$\varepsilon_{0,a}$(%)	ε_m(%)	T_c(0) (K)	B_{c2}(0,0) (T)	F_m(0,0) (AT)
100 h						
0.697	2.266	0.296	0.305	16.50	31.65	24,884
73.32	33.18					
150 h						
0.725	2.336	0.333	0.288	16.57	31.97	27,374
68.19	28.42					

Table 4
Fitting parameters obtained with Eq. (4) for samples 100 h and 150 h.

p	q	n	ε_m(%)	T_c(0)	B_{c2}(0,0)	A(0)
v	w	u		c_2	c_3	c_4
100 h						
0.630	2.298	2.354	0.303	16.95	34.24	22,721
1.306	2.599	−0.114		−1.008	−1.1938	−0.5923
150 h						
0.667	2.420	2.418	0.289	17.21	34.68	25,922
1.296	2.161	−0.240		−0.775	−0.7827	−3.643

The interpolative scaling law is also related with the Kramer model and microscopic theory [10] and can be simplified as,

$$I_c(B,T,\varepsilon) = A(\varepsilon)[T_c(\varepsilon)(1-t^2)]^2[B_{c2}(T,\varepsilon)]^{n-3}b^{p-1}(1-b)^q \quad (4)$$

The temperature dependence of the upper critical field can be written as, $B_{c2}(T,\varepsilon) = B_{c2}(0,\varepsilon)(1-t^v)$ and the strain dependence is described by the following polynomial function:

$$B_{c2}(0,\varepsilon)/B_{c2}(0,0) = 1 + c_2\varepsilon^2 + c_3\varepsilon^3 + c_4\varepsilon^4$$

The strain dependences of the upper critical field and the transition temperature are related to each other as, $B_{c2}(0,\varepsilon)/B_{c2}(0,0) = [T_c(\varepsilon)/T_c(0)]^w$, as was suggested by Ekin [15]. The function $A(\varepsilon)$ is almost proportional to the pinning force maximum when the variation in the transition temperature and the upper critical field is small and has a correlation with the transition temperature, $A(\varepsilon)/A(0) = [T_c(\varepsilon)/T_c(0)]^u$. The fitting results are listed in Table 4. The calculated critical current curves were quite similar to the thick solid lines in Fig. 2. (To avoid complication, they are not shown in Fig. 2.) Here again, similar trends are observed; the polynomial strain dependency coefficients (c_2, c_3 and c_4) decrease, the transition temperature slightly increases, and $A(0)$ increases significantly with the longer duration time at the A15 reaction temperature.

4. Conclusions

In summary, detailed critical current measurements have been carried out for internal-tin Nb_3Sn strands with different heat treatment scenarios. It is found that 50 h of additional heat treatment at the A15 reaction temperature can greatly reduce the strain dependence of the critical current compared with 100-h long heat treatment, especially in the compressive strain region. The measured results were analyzed with the scaling law based on the strong-coupling theory of superconductivity, the modified deviatoric strain scaling law, and the interpolative scaling law. All the analyses indicate that the critical temperature or the upper critical field slightly increases whereas the pinning force maximum strongly increases with 50 h of additional heat treatment at 650 °C. The origin of the improved strain dependency is discussed in terms of the reduction of the Ginzburg–Landau parameter strain dependency coefficient γ, which is related to the change in the impurity scattering rate. Or it may be due to the decreases in the second and third invariant axial strain coefficients according to the analysis based on the modified deviatoric strain scaling law.

Acknowledgments

This work was supported by the Korea Ministry of Science and Technology of Republic of Korea under the ITER Project Contract, in part by a Korea Science and Engineering Foundation (KOSEF) Grant funded by the Korean Government (MEST) (No. R01-2007-000-20462-0).

References

[1] A. Godeke, Supercond. Sci. Technol. 19 (2006) R68.
[2] R. Flükiger, D. Uglietti, C. Senatore, F. Buta, Cryogenics 48 (2008) 293.
[3] J. Kim, K. Sim, K. Jang, S. Je, P. Park, S. Oh, K. Kim, IEEE Trans. Appl. Supercond. 18 (2008) 1043.
[4] H. Fillunger, M. Foitl, K. Hense, I. Kajgana, A. Kasztler, H. Kirchmayr, R. Lackner, J. Lackner, J. Leoni, R. Maix, M. Müller, IEEE Trans. Appl. Supercond. 12 (2008) 1049.
[5] H. Müller, Th. Schneider, Cryogenics 48 (2008) 323.
[6] N. Mitchell, Cryogenics 43 (2003) 255.
[7] S. Oh, S. Park, C. Lee, Y. Chang, K. Kim, P. Park, IEEE Trans. Appl. Supercond. 15 (2005) 3462.
[8] S. Oh, C. Lee, H. Choi, K. Moon, K. Kim, J. Kim, P. Park, IEEE Trans. Appl. Supercond. 18 (2008) 1063.
[9] S. Oh, K. Kim, J. Appl. Phys. 99 (2006) 033909.
[10] D. Taylor, D. Hampshire, Supercond. Sci. Technol. 18 (2005) S241.
[11] A. Godeke, B. ten Haken, H. ten Kate, D. Larbalestier, Supercond. Sci. Technol. 19 (2006) R100.
[12] E. Kramer, J. Appl. Phys. 44 (1973) 1360.
[13] S. Oh, C. Lee, K. Cho, K. Kim, D. Uglietti, R. Flükiger, Supercond. Sci. Technol. 20 (2007) 851.
[14] L. Bottura, B. Bordini, IEEE Trans. Appl. Supercond. 19 (2009) 1521.
[15] J.W. Ekin, Cryogenics 20 (1980) 611.